Ratiometric luminescence detection of copper(I) by a resonant system comprising two antenna/lanthanide pairs

Céline Cepeda, Sergey A. Denisov, Didier Boturyn, Nathan D. Mcclenaghan, Olivier Sénèque

Ratiometric Luminescence Detection of Copper(I) by a Resonant System Comprising Two Antenna / Lanthanide pairs

Céline Cepeda, Sergey A. Denisov, Didier Boturyn, Nathan D. McClenaghan,* Olivier Sénèque*

Corresponding authors

Olivier Sénèque

Univ. Grenoble Alpes, CNRS, CEA, IRIG, LCBM (UMR 5249), 38000 Grenoble, France; ORCID: 0000-0002-0633-5528; Email: *olivier.seneque@cea.fr*

Nathan D. McClenaghan

Univ. Bordeaux, CNRS, ISM (UMR 5255), 33405 Talence, France; ORCID: 0000-0003-0285-1741

Authors

Celine Cepeda

Univ. Grenoble Alpes, CNRS, CEA, IRIG, LCBM (UMR 5249), 38000 Grenoble, France; Univ. Grenoble Alpes, CNRS, DCM (UMR 5250), 38000 Grenoble, France

Sergey A. Denisov

Univ. Bordeaux, CNRS, ISM (UMR 5255), 33405 Talence, France; Present address: Univ. Paris-Saclay, CNRS, ICP (UMR 8000), 91405 Orsay, France; ORCID: 0000-0001-7881-1979

Didier Boturyn

Univ. Grenoble Alpes, CNRS, DCM (UMR 5250), 38000 Grenoble, France; ORCID: 0000-0003-2530-0299

Abstract

Selective and sensitive detection of Cu(I) is an ongoing challenge due to its important role in biological systems, for example. Herein, we describe a photoluminescent molecular chemosensor integrating two lanthanide ions (Tb^{3+} and Eu^{3+}) and respective tryptophan and naphthalene antennas onto a polypeptide backbone. The latter was structurally inspired from copper-regulating biomacromolecules in gram negative bacteria and was found to bind Cu^{+} effectively in pseudobiological conditions (log K_{Cu+} = 9.7 ± 0.2). Ion regulated modulation of lanthanide luminescence in terms of intensity and long, millisecond lifetime offers perspectives in terms of ratiometric and time-gated detection of Cu^{+}. Role of the bound ion in determining the photophysical properties is discussed with the aid of additional model compounds.

Keywords

Peptide – Lanthanide – Copper – Luminescence – Probe

Introduction

Copper is an essential trace element for most living organisms,[1,2] where it exists in two stable oxidation states: +I in the reducing cellular environment and +II in the extracellular environment. Indeed, Cu serves as a redox-active cofactor in several proteins. Copper is distributed between an inert pool, tightly bound to proteins, and a labile pool, which corresponds to copper ions experiencing dynamic exchange between proteins or small molecules (e.g. glutathione or cysteine). Despite being required for life, copper can also be toxic in an aerobic environment because of Fenton-like reactions, which can catalyze production of reactive oxygen species. Therefore, homeostasis of copper is tightly regulated. Copper trafficking within cells relies on various proteins dedicated to copper uptake, transport and export.[3,4] Copper imbalance can be associated to severe diseases (e.g. Menkes diseases,[5] Wilson disease,[6] neurodegenerative diseases[7] or cancers[8]). The importance of copper in biology has prompted the development of fluorescent sensors for labile Cu^+ monitoring in cells.[9–13] Two kinds of copper-responsive sensors have been explored: activity-based or recognition-based.[10] In the former case, the sensor reacts irreversibly with Cu^+ to yield a fluorescent molecule. It is well suited to signal the presence, even transiently, of Cu^+. However, once the sensor is activated, the signal remains constant, even if Cu^+ in the medium is removed. For recognition-based sensors, reversible binding of Cu^+ to chelating groups of the sensor turns fluorescence off or on. Such a sensor is suitable to monitor the dynamics of exchangeable Cu^+. Despite intense research endeavors to design suitable recognition-base Cu^+ sensors, the ideal Cu^+-responsive fluorescent probe remains elusive. Besides selectivity, such a probe must have a strong affinity for Cu^+ as this cation is buffered in the femtomolar range in normal cells. For quantification purposes in non-homogenous biological samples, a ratiometric sensor is required. A ratiometric fluorescent probe displays excitation or emission spectral changes upon Cu^+ binding. However, ratiometric probes are more difficult to design than intensiometric ones, for which Cu^+ binding increases or decreases the fluorescence intensity without modifying the emission spectrum. As a consequence, many Cu^+-responsive intensiometric probes have been described and examples of ratiometric Cu^+ fluorescent probes remain scarce.[14–16]

We are interested in developing luminescent probes for metal cations or biomolecules based on peptides and luminescent trivalent lanthanides (Ln^{3+}).[17–22] Lanthanides display desirable luminescent properties for biological applications, which comprise: (i) line-like emission bands ranging from the visible to the near infrared (NIR), (ii) large Stokes shift, (iii) long luminescence lifetimes (allowing suppression of background fluorescence in time-resolved detection) and (iv) excellent photostability.[23–27] Because f-f transitions are forbidden by the Laporte rules, direct excitation of Ln^{3+} is inefficient ($\varepsilon < 10\ M^{-1}\ cm^{-1}$). Efficient lanthanide luminescence relies on the so-called "antenna effect": an organic chromophore (the antenna) is used as a light-harvesting device to transfer, after excitation, electronic energy to the Ln^{3+} in order to populate its emissive excited state. There are many possibilities to modulate the luminescence of lanthanide complexes. This has prompted the design of responsive probes able to detect various bioanalytes based on lanthanide complexes.[28–31] In the luminescent probes we have developed, the peptide serves as a recognition unit for the analyte of interest. We have described a Cu^+-responsive luminescent probe, **LCC1^{Tb}** (Figure 1A), inspired from the protein CusF, a Cu^+-trafficking protein in gram negative bacteria.[32,33] This probe is composed of an 18-amino acid cyclic peptide featuring two methionine, one histidine and a tryptophan as Cu^+ coordination set and a DOTA[Tb] complex as a luminescent unit.[20,21] The tryptophan serves also as an antenna for Tb^{3+} luminescence. **LCC1^{Tb}** binds one Cu^+, selectively among other biological cations due to the thioether side chains of the methionines.[34,35] In the Cu^+-bound form, the tryptophan side chain is engaged in a cation/π interaction with Cu^+ (Figure 1C), which enhances the antenna effect, resulting in an increased Tb^{3+} emission.[20] In order to improve this Cu^+-responsive probe, we targeted ratiometric Cu^+ detection.

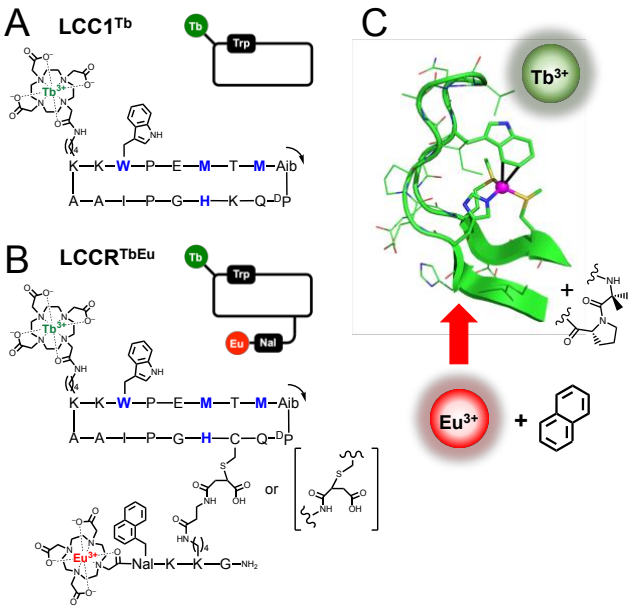

Figure 1. (A,B) Chemical structure and schematic representation of (A) **LCC1^{Tb}** and (B) **LCCR^{TbEu}**, Cu-chelating amino acids in blue and black. Arrow indicates the N–to–C direction within the cyclic peptide. Nal = 3-(1-naphthyl)-L-alanine; Aib = 2-aminoisobutyric acid; ^{D}P = D-proline. (C) Cu^{+} binding site of CusF (pdb 2VB2[36]) and design principle showing the positioning of the various components.

We have recently reported that ratiometric Zn^{2+}-responsive probes may be obtained by functionalizing a zinc finger peptide with two distinct Ln complexes and a single antenna capable of sensitizing both Ln^{3+}.[19] In this system, the emission intensity of one of the Ln^{3+} is strongly increased upon Zn^{2+} binding, while that of the other barely changes. Two ratiometric probes were described, one emitting in the visible thanks to a Tb^{3+} / Eu^{3+} pair and the other one emitting in the NIR with an Yb^{3+} / Nd^{3+} pair. Such a ratiometric system requires inert Ln complexes in order to avoid scrambling of the two Ln^{3+}, which was warranted by the use of DOTA[Ln] complexes. However, because all Ln^{3+} have almost the same coordination properties, selective metalation of the two DOTA ligands has to be controlled. This was achieved by synthesizing the probe through native chemical ligation of two peptide segments, each bearing a distinct DOTA[Ln] complex. In this article, we explore a second strategy to design Ln-based ratiometric sensors, applied to the Cu^{+} case. It relies on the use of two distinct antenna / Ln couples rather than on a single antenna for two Ln. In this respect, a remote naphthalene / DOTA[Eu] couple was appended to **LCC1^{Tb}**. The new probe, **LCCR^{TbEu}** (Figure 1B), displays a ratiometric response to Cu^{+}, but unlike **LCC1^{Tb}** that shows a strong enhancement of Tb^{3+} emission upon Cu^{+} binding, **LCCR^{TbEu}** shows only a modest increase of Tb^{3+} emission and a stronger increase of Eu^{3+} emission. This behavior is rationalized by the study of several variants lacking one or several key components among the naphthalene antenna and the two Ln emitters.

Results and discussion

Probe design and synthesis. In order to design a ratiometric probe starting from **LCC1^{Tb}**, Eu^{3+} was chosen as a second Ln emitter. Tb^{3+} has four major emission bands at 490, 540, 585 and 623 nm, corresponding to $^{5}D_4 \rightarrow {}^{7}F_J$ (J = 6, 5, 4 and 3) transitions, respectively, while Eu^{3+} has five major emission bands at 580, 590, 615, 750 and 700 nm, corresponding to $^{5}D_0 \rightarrow {}^{7}F_J$ (J = 0, 1, 2, 3 and 4), respectively. Their emission spectra overlap in the 570-630 nm window but distinct bands can readily be used to monitor Tb^{3+} emission at 490 and 540 nm and Eu^{3+} at

700 nm. Tryptophan is not a suitable antenna for Eu^{3+},[37] therefore, we opted for naphthalene, an efficient Eu^{3+} sensitizer.[38–40] Like tryptophan, naphthalene has a π-π* transition around 280 nm, so both antennas can be excited at the same wavelength (Figure S7 of SI). As mentioned above, in order to avoid Ln^{3+} scrambling, we chose to use two DOTA[Ln] complexes within the probe. Construction of the probe could be envisioned by thiol/maleimide ligation of: (i) a cyclic peptide mostly resembling the parent probe **LCC1^{Tb}** but containing a cysteine and (ii) a second peptide comprising a DOTA[Eu] complex and a 3-(1-naphthyl)-L-alanine amino acid as well as a maleimide group. For the cyclic peptide, the cysteine was introduced in place of the lysine next to the histidine of **LCC1^{Tb}** (Figure 1A),[20] in order that its side chain points in the opposite direction to the Cu^{+}-binding site (Figure 1). The synthesis of the cyclic fragment, **1^{Tb}** (Figure 2), is described in the Supporting Information (SI). Briefly, the synthesis was performed as follows: (i) a linear precursor with a N-terminal protected cysteine was assembled on SEA-PS ((*bis*(2-sulfanylethyl)-amino)-2-chlorotrityl-polystyrene) resin, (ii) a *t*Bu-protected DOTA ligand was coupled to a lysine side chain, after selective removal of its alloc protecting group using Pd^{0}, (iii) the peptide was cleaved from the resin and protecting group were removed under acidic conditions, (iv) the peptide was dissolved in phosphate buffer pH 7.0 containing TCEP (*tris*(2-carboxyethyl)phosphine) and MPAA (4-mercaptophenylacetic acid) to trigger cyclization by SEA native chemical ligation[41–43] and (v) metalation with Tb^{3+} in water afforded **1^{Tb}**. For the Eu^{3+} and naphthalene-containing fragment, peptide **2Nal** (Figure 2) was synthesized (details are given in the SI) but during metalation with Eu^{3+} in water (pH 6.2), hydrolysis of the maleimide group was observed and **3Nal^{Eu}** was obtained. Nevertheless, ligation of **1^{Tb}** and **3Nal^{Eu}** could be achieved in phosphate buffer (pH 7.5) at room temperature and was completed within 15-24 h. As displayed in Figure 1A (bottom), two regioisomers can be obtained after the thiol/maleamide ligation, but HPLC purification gave a single peak for **LCCR^{TbEu}**, indicating the presence of a single, non-identified, isomer or of both isomers that cannot be resolved by HPLC.

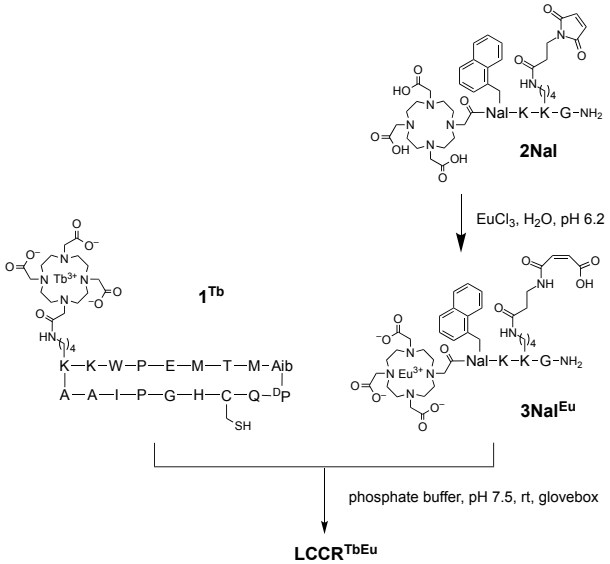

Figure 2. Synthesis of **LCCR^{TbEu}**.

Spectroscopic characterization of LCCR^{TbEu}. The luminescence properties of **LCCR^{TbEu}** in response to Cu^{+} were investigated in HEPES buffer (10 mM, pH 7.5). In order to maintain Cu in the +I oxidation state, solutions were prepared in anaerobic conditions using a glovebox and the buffer contained hydroxylamine (20 mM) as a reducing agent. Cu^{+} was generated *in situ* by addition of $CuSO_4$ dissolved in water. Excitation of **LCCR^{TbEu}** was performed at 280 nm. The free peptide displays a tryptophan-like fluorescence emission with a maximum at 355 nm. The fluorescence intensity decreases proportionally to the amount of added Cu^{+} up to 1.0

eq. and remains constant above this limit (Figure S8 of SI). This indicates the formation of a tightly-bound 1:1 complex between Cu^+ and **LCCR^{TbEu}**, as observed for **LCC1^{Tb}**. Formation of this complex results in a 42 % quench of the initial fluorescence. The time-gated (100 µs delay) emission spectrum of **LCCR^{TbEu}** displays both Tb^{3+} and Eu^{3+} emission in comparable intensities: the intensity of the Eu^{3+} $^5D_0 \rightarrow {}^7F_4$ transition at 702 nm is 1.35 times that of the Tb^{3+} $^5D_4 \rightarrow {}^7F_1$ transition at 545 nm (Figure 3A). Upon addition of Cu^+, both Tb^{3+} and Eu^{3+} emission increase up to 1.0 eq. (Figure 3B), confirming the formation of the Cu·**LCCR^{TbEu}** complex. Surprisingly with respect to **LCC1^{Tb}**, that displays a large enhancement of Tb^{3+} emission (×6) due to the cation-π interaction that is established between tryptophan and Cu^+, the increase of Tb^{3+} emission is rather modest (×1.35). However, the increase of Eu^{3+} emission is bigger (×3.15). This differential enhancement makes **LCCR^{TbEu}** a ratiometric probe for Cu^+: the ratio of the intensity measured at 702 nm (Eu^{3+}) over the one at 545 nm (Tb^{3+}), I_{702}/I_{545}, permits monitoring of the formation of the Cu·**LCCR^{TbEu}** complex (Figure 3C). The luminescence lifetimes (τ_{Ln}) of both lanthanides were measured during the titration. That of Eu^{3+} decreases slightly from 0.67 ms to 0.61 ms. These values are typical of a mono-hydrated Eu^{3+}-DOTA-monoamide complex.[17,18] More interestingly, the value of τ_{Tb} for is **LCCR^{TbEu}** 0.89 ms, which is much shorter than the one of **LCC1^{Tb}**, 1.98 ms,[20] typical of mono-hydrated Tb^{3+}-DOTA-monoamide complexes.[17,44] Nevertheless, determination of the hydration number (q) of Tb^{3+} and Eu^{3+} evidenced a single Ln-bound water molecule for both lanthanides, as expected with the DOTA-monoamide ligand (details in the SI). During the Cu^+ titration, τ_{Tb} increases from 0.89 ms to 0.98 ms, a value reached at 1.0 eq. Cu^+ that remains constant in presence of excess Cu^+ (Figure 3D). Hence, Cu^+ binding can be monitored following τ_{Tb}. **LCCR^{TbEu}** behaves also as a lifetime probe for Cu^+. Note that lifetime sensing is also intrinsically ratiometric.

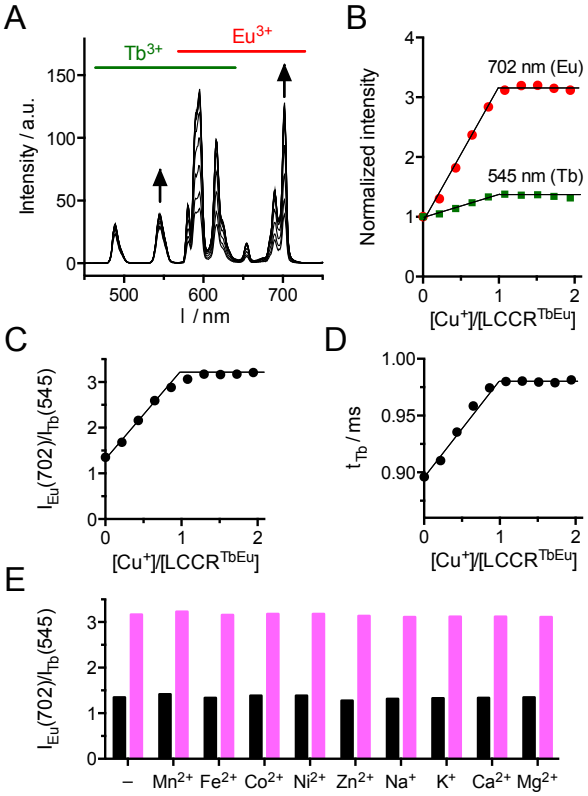

Figure 3. Luminescence response of **LCCR^{TbEu}** to Cu^+. (A–D) Titration of **LCCR^{TbEu}** by Cu^+ showing (A) the sensitized time-gated luminescence emission spectra (λ_{ex} = 280 nm, delay = 100 µs), (B) the evolution of the Tb^{3+} (545 nm, green square) and Eu^{3+} emissions (702 nm, red dot) against the metal/probe ratio; (C) the evolution of I_{702}/I_{545} , corresponding to the intensity ratio of the Eu^{3+} and Tb^{3+} channels and (D) the evolution of the Tb^{3+}

luminescence lifetime. (E) Selectivity diagram showing the I_{702}/I_{545} for **LCCR^{TbEu}** (5 µM) in the absence (black) and presence (pink) of Cu^{+} (10 µM) after addition of various cations: Mn^{2+}, Fe^{2+}, Co^{2+}, Ni^{2+}, Zn^{2+} (10 µM), Na^{+}, K^{+} (50 mM), Mg^{2+}, Ca^{2+} (10 mM). Solutions were prepared anaerobically in HEPES buffer (10 mM, pH 7.5) containing NH_2OH (20 mM).

Among physiological cations, **LCC1^{Tb}** is only able to bind Cu^{+}. However, it also responds to the non-physiological Ag^{+} ion, which has coordination properties very similar to those of Cu^{+} with biological ligands. The selectivity of **LCCR^{TbEu}** for Cu^{+} *vs* other physiological cations (Na^{+}, K^{+}, Ca^{2+}, Mg^{2+}, Mn^{2+}, Fe^{2+}, Co^{2+}, Ni^{2+}, Zn^{2+}) was investigated. Figure 3E shows the values of the ratio I_{702}/I_{545} for **LCCR^{TbEu}** and Cu·**LCCR^{TbEu}** in the presence of various cations. Clearly, among physiological cations, **LCCR^{TbEu}** responds to Cu^{+} only. The behavior of **LCCR^{TbEu}** was also investigated with Ag^{+} under both anaerobic (argon) and aerobic (air-equilibrated solution) conditions (HEPES buffer, 10 mM, pH 7.5). Not surprisingly, **LCCR^{TbEu}** responds ratiometrically to Ag^{+} in a similar way as to Cu^{+} with only slight differences as shown in Figure 4. It is interesting to note that in all cases, (i) the metal-induced enhancement of emission is stronger for Eu^{3+} than for Tb^{3+}, leading to an increase of I_{702}/I_{545} upon metal binding and (ii) the Tb^{3+} lifetime (ca. 1 ms) is shorter than that of **LCC1^{Tb}** and it increases upon metal binding. Finally, the binding constant of Cu^{+} and Ag^{+} by **LCCR^{TbEu}** were determined (details in the SI). Cu^{+} binding is tighter than Ag^{+}: log K_{Cu+} = 9.7 ± 0.2 and log K_{Ag+} = 7.1 ± 0.2. These values are comparable to those obtained for other members of this family of probe.[20,21]

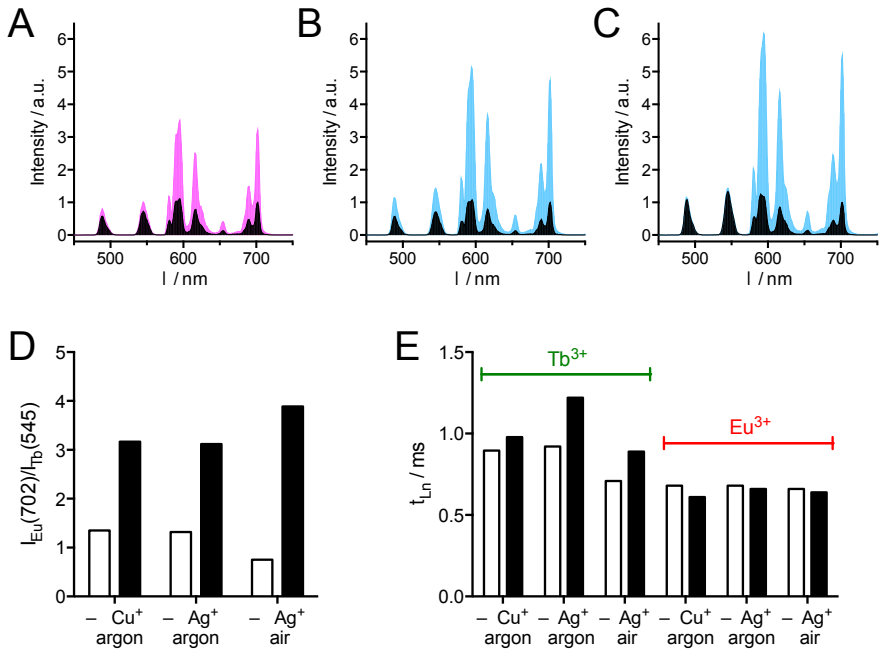

Figure 4. Comparison of luminescence response of **LCCR^{TbEu}** to Cu^{+} and Ag^{+} in anaerobic conditions (argon) as well as to Ag^{+} in aerobic conditions (air). (A–C) Time-gated emission spectra (λ_{ex} = 280 nm, delay = 100 µs) of **LCCR^{TbEu}** (black) and its Cu^{+} (pink) and Ag^{+} (blue) complexes: (A) Cu^{+} / argon, (B) Ag^{+} / argon, (C) Ag^{+} / air. The spectrum of free **LCCR^{TbEu}** was normalized to the intensity at 702 nm. (D) ratio I_{702}/I_{545} = I(Eu)/I(Tb) for **LCCR^{TbEu}** (white bars) and its complexes (black bars) in the various conditions (Cu^{+} / Ag^{+}, argon / air). (E) Ln^{3+} luminescence lifetimes (τ_{Ln}) of **LCCR^{TbEu}** (white bars) and its complexes (black bars) in the various conditions (Cu^{+} / Ag^{+}, argon / air). Solutions were prepared anaerobically in HEPES buffer (10 mM, pH 7.5) containing NH_2OH (20 mM).

Mechanistic insight into the behavior of LCCR^{TbEu}. LCCR^{TbEu} was built by adding a short peptide tail to **LCC1^{Tb}**. The tail, comprising a DOTA[Eu] complex and its naphthalene antenna, was appended on **LCC1^{Tb}** so as to be relatively far from the DOTA[Tb] / tryptophan pair in the folded state (Figure 1B) even if there is a degree of intrinsic conformational flexibility of this tail. As shown above, **LCCR^{TbEu}** behaves as a ratiometric probe for Cu^+ or Ag^+. However, unlike **LCC1^{Tb}** that shows a strong enhancement of Tb^{3+} emission upon Cu^+ binding upon 280 nm excitation, **LCCR^{TbEu}** shows a small enhancement of the Tb^{3+} emission but a much stronger enhancement of the Eu^{3+} emission. A particularly short Tb^{3+} luminescence lifetime for a DOTA[Tb] complex also characterizes **LCCR^{TbEu}**, which indicates an extra deexcitation pathway for its DOTA[Tb] complex compared to **LCC1^{Tb}**. For the latter, we have demonstrated that the cation-π interaction established upon Cu^+ or Ag^+ binding increases intersystem crossing (ISC) within the tryptophan resulting in a higher population of its triplet state, which is the donor state in the electronic energy transfer to the $^5D_4$ excited state of Tb^{3+}.[20] Therefore, population of the Tb^{3+} $^5D_4$ excited state is higher in the Cu^+ or Ag^+-bound form, leading to more intense Tb^{3+} emission. Formation of the cation-π interaction could be evidenced by a red-shift of the tryptophan π-π* transition.[20,36] Interestingly, in the case of **LCCR^{TbEu}**, the excitation spectrum of Tb^{3+} is red-shifted upon Cu^+ or Ag^+ binding as is that of Eu^{3+} (Figure S11 of ESI). This indicates that, at least in part, Eu^{3+} sensitization originates from photons absorbed by the tryptophan. However, Horrocks demonstrated that tryptophan cannot sensitize Eu^{3+} luminescence.[37] This implies that either the cation-π interaction makes tryptophan a suitable antenna for Eu^{3+} or some electronic energy transfer (EET) occurs between the two antenna / Ln^{3+} pairs.

A simplified Jablonski-Perrin diagram for **LCCR^{TbEu}** is shown in Figure 5. Tryptophan and naphthalene singlet excited states (S_1) are located at 32 000 and 31 000 cm^{-1}, respectively and their triplet excited states (T_1) lie at 24 100 and 21 100 cm^{-1}, respectively.[45–47] Due to the small energy difference between the two S_1 states, bi-directional EET is possible between them (blue arrow #1 in Figure 5). Since the cation-π interaction increases ISC in the tryptophan, resulting in an enhanced T_1 population,[20,48] triplet-triplet EET between tryptophan and naphthalene (blue arrow #2) can be considered as well. The $^5D_4$ excited state of Tb^{3+} is located at 20 400 cm^{-1} and the $^5D_0$, $^5D_1$ and $^5D_2$ excited states of Eu^{3+} at 17 250, 19 000 and 21 450 cm^{-1}, respectively. Naphthalene is known to sensitize Eu^{3+} via EET from its T_1 state and bidirectional EET between naphthalene(T1) and Tb^{3+}($^5D_4$) (blue arrow #3), which are almost isoenergetic, is also possible.[40] As mentioned above, due to the cation-π interaction, sensitization of Eu^{3+} by tryptophan cannot be ruled out here (blue arrow #4) (*Note:* sensitization of Eu^{3+} from tryptophan(S_1) could be considered as well, but this EET is not represented in Figure 5). Finally, direct $Tb^{3+} \rightarrow Eu^{3+}$ EET can be effective up to 15-20 Å and can be considered here due to the flexibility of the molecule that does not guarantee that the two Ln^{3+} are always separated by longer distances.[49]

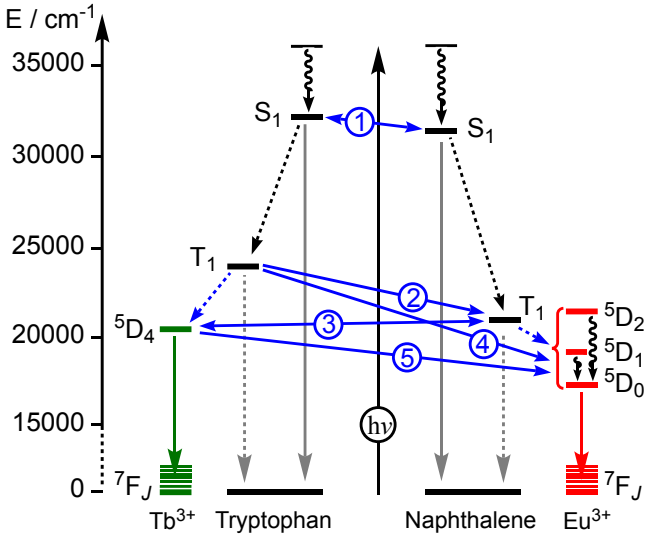

Figure 5. Simplified Jablonski-Perrin diagram for **LCCR^{TbEu}** showing pertinent photophysical processes: absorption (solid black arrow), intersystem crossing (dashed black arrows), fluorescence (solid grey arrows), phosphorescence (dashed grey arrows), Tb^{3+} (green arrow) and Eu^{3+} (red arrow) luminescence and electronic energy transfer (blue arrows).

In order to determine which EET processes are effectively at play, several variants of **LCCR^{TbEu}** were studied, lacking one or several of the chromophores among naphthalene, Tb^{3+} and Eu^{3+}. The tryptophan was always present in these variants because it acts as one of the Cu^{+} / Ag^{+} ligands, being engaged in the cation-π interaction with these cations. For variants lacking the naphthalene, the 3-(1-naphthyl)-L-alanine was replaced by L-alanine. For variants lacking Tb^{3+} or Eu^{3+}, the Ln^{3+} was replaced by Gd^{3+} in order to fill the DOTA chelate. Gd^{3+} cannot be sensitized by tryptophan or naphthalene because its excited states are too high in energy: it acts as a spectator in the corresponding variants. Three variants were synthesized with the naphthalene, **LCCR^{TbGd}**, **LCCR^{GdEu}** and **LCCR^{GdGd}**, as well as three others without the naphthalene, **LCCΔ^{TbEu}**, **LCCΔ^{GdEu}** and **LCCΔ^{TbGd}**. Their synthesis is described in the SI. As **LCCR^{TbEu}** behaves similarly with Cu^{+} and Ag^{+}, these molecules were studied with Ag^{+} because it allows measurements in both aerobic and anaerobic conditions, in order to unveil possible involvement of T_1 states, which can be sensitive to O_2. All measurements were performed in HEPES buffer as mentioned above and the same acquisition parameters of the spectrometer were used to record spectra in order to compare emitted intensities of pairs of molecules.

First, we examined if besides naphthalene and Eu^{3+} other tail components could alter the Ag^{+} response by comparing **LCC1^{Tb}** and **LCCΔ^{TbGd}**, lacking both naphthalene and europium. Both probes have comparable emitted Tb^{3+} intensities in the absence of Ag^{+} and they show the same enhancement of Tb^{3+} luminescence upon Ag^{+} binding, both under air or argon (Figure 6A). The Tb^{3+} luminescence lifetime is ca. 1.95 ms for both probes. This indicates that, apart from naphthalene and Eu^{3+}, the tail has no influence on the probe behavior. Next, we investigated if the cation-π interaction could convert the tryptophan into an efficient antenna for Eu^{3+}. For this purpose, **LCCR^{TbEu}** and **LCCΔ^{GdEu}** were compared. Figure 6B compares the intensity of Eu^{3+} emission at 702 nm (λ_{ex} = 280 nm) for both probes in their Ag^{+}-free and Ag^{+}-bound forms in anaerobic conditions. Eu^{3+} emission of the variant is more than 1000 times lower than that of **LCCR^{TbEu}**, demonstrating that tryptophan is not an efficient antenna for Eu^{3+}, even when it is engaged in a cation-π interaction. This was corroborated with **LCC1^{Eu}**, the Eu^{3+} analogue of **LCC1^{Tb}**, for which the Eu^{3+} emission is hardly detected in both free and Cu^{+} or Ag^{+}-bound forms. Therefore, tryptophan(T_1) → Eu^{3+}(^5D_J) EET (#4 in Figure 5) are not efficient and should not be considered. Next, we examined if direct EET between Tb^{3+} and Eu^{3+} excited states could be efficient with variants of **LCCΔ^{TbEu}**,

lacking only the naphthalene in comparison with **LCCR^{TbEu}**. **LCCΔ^{TbEu}** behaves basically like **LCC1^{Tb}**, including a red-shifted π-π* transition and a large Tb^{3+} luminescence enhancement upon Ag^{+} or Cu^{+} binding, but with a very weak additional Eu^{3+} emission. The Eu^{3+} emission of **LCCΔ^{TbEu}** in its Ag^{+}-free and Ag^{+}-bound forms corresponds to 1.4 % and 0.9 %, respectively, of that of **LCCR^{TbEu}** in anaerobic conditions (Figure 6C). In aerated solutions, these relative values are a little bit higher (6 % and 1.7 %, respectively) but still very low. As tryptophan is not able to sensitize Eu^{3+}, this suggests that direct $Tb^{3+}(^5D_4) \rightarrow Eu^{3+}(^5D_J)$ EET (#5 in Figure 5) is not efficient. This is confirmed by the Tb^{3+} luminescence lifetime which is 1.95 ± 0.02 ms for both **LCCΔ^{TbEu}** and Ag·**LCCΔ^{TbEu}**, both in aerobic and anaerobic conditions. Hence, direct $Tb^{3+}(^5D_4) \rightarrow Eu^{3+}(^5D_J)$ EET should not be considered an important process.

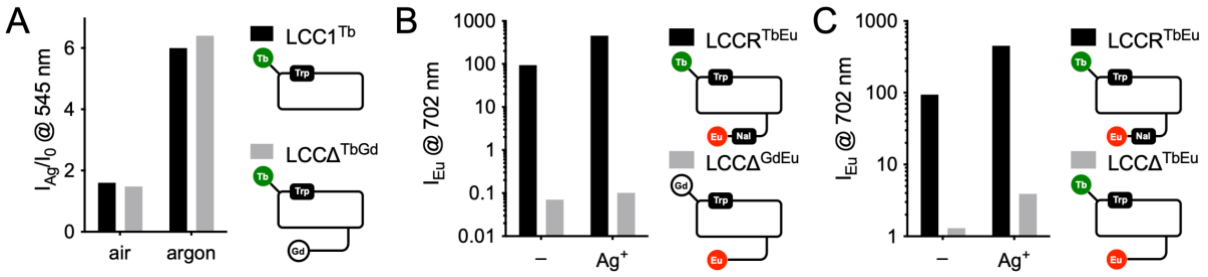

Figure 6. Comparative behavior of naphthalene-lacking **LCCΔ^{Ln1Ln2}** probes. (A) Comparison of time gated Tb^{3+} luminescence enhancement (I_{Ag}/I_0) at 545 nm upon Ag^{+} binding between **LCC1^{Tb}** (black) and **LCCΔ^{TbGd}** (grey) in aerobic and anaerobic conditions. (B) Comparison of time gated Eu^{3+} luminescence (702 nm) between **LCCR^{TbEu}** (black) and **LCCΔ^{GdEu}** (grey) in their Ag^{+}-free and Ag^{+}-bound forms. (C) Comparison of time gated Eu^{3+} luminescence (702 nm) between **LCCR^{TbEu}** (black) and **LCCΔ^{TbEu}** (grey) in their Ag^{+}-free and Ag^{+}-bound forms. Solutions were prepared in HEPES buffer (10 mM, pH 7.5); λ_{ex} = 280 nm.

Results obtained with **LCCΔ^{Ln1Ln2}** probes point to an essential role of the naphthalene moiety in **LCCR^{TbEu}**. Importantly, Faulkner et al. have shown that naphthalene can be used as sensitizing antenna for both Tb^{3+} and Eu^{3+} in hetero-bis(lanthanide) systems but that thermal repopulation of naphthalene(T_1) from $Tb^{3+}(^5D_4)$ arises in such a system.[40] The next molecule to be studied was **LCCR^{TbGd}** that features the naphthalene chromophore in the tail but not the Eu^{3+} ion. Its emission properties were compared to **LCC1^{Tb}** to assess the effect of the naphthalene (Figure 7). In aerated solution, the Tb^{3+} emission intensity of **LCCR^{TbGd}** is slightly lower than that of **LCC1^{Tb}** but Ag^{+} addition does not induce any increase of Tb^{3+} emission, unlike **LCC1^{Tb}** (×1.6). In anaerobic conditions, the Tb^{3+} emission of **LCCR^{TbGd}** is 7 times higher than for **LCC1^{Tb}** in the free-form and Ag^{+} induces only a modest 15 % enhancement of Tb^{3+} emission compared to 500 % for **LCC1^{Tb}**. As for **LCCR^{TbEu}**, the Tb^{3+} luminescence lifetimes of **LCCR^{TbGd}** are shorter (0.68 ms (free) and 0.86 ms (Ag^{+}) in aerobic conditions and 1.32 ms (free) and 1.33 ms (Ag^{+}) in anaerobic conditions) than those of **LCC1^{Tb}** (ca. 1.9 ms).[20] All this indicates that adding a naphthalene moiety to **LCC1^{Tb}** has a dramatic effect on the luminescence behavior and perturbates the tryptophan / Tb^{3+} pair by acting as a second sensitizing antenna for Tb^{3+} but also by adding a novel deexcitation pathway for the $Tb^{3+}(^5D_4)$ state through the naphthalene(T_1) state as evidenced by the low $^5D_4$ decay time compared to **LCC1^{Tb}** and its oxygen dependence. In order to confirm that $Tb^{3+}(^5D_4) \rightarrow$ naphthalene(T_1) EET can occur in this system, the Tb^{3+} ion in **LCCR^{TbEu}** was excited directly through the $^7F_6$-$^5D_4$ f-f transition at 488 nm. Emission of both Tb^{3+} and Eu^{3+} was detected and their proportion in the emission spectrum is similar to the one obtained while exciting into the π-π* transition of the antennas at 280 nm (Figure S12 of SI). Excitation of Cu·**LCCΔ^{TbEu}** or Ag·**LCCΔ^{TbEu}** at 280 nm resulted also in emission of both Tb^{3+} and Eu^{3+}, still in proportions comparable to those obtained with 280 nm excitation (Figure S12 of SI). Comparatively, excitation of **LCCΔ^{TbEu}** at 488 nm

resulted in Tb^{3+} emission only, demonstrating again that direct energy transfer from Tb^{3+} to Eu^{3+} is inefficient. From this, we can conclude that naphthalene(T_1) serves as an energy relay between Tb^{3+} and Eu^{3+}. The similar proportion of Tb^{3+} and Eu^{3+} in emission spectra upon excitation at 280 nm or 488 nm suggests that the relative intensity of Tb^{3+} and Eu^{3+} emission is mainly governed by the relative rate constants of (i) forward and back energy transfer between $Tb^{3+}(^5D_4)$ and naphthalene(T_1) and (ii) naphthalene(T_1) → $Eu^{3+}(^5D_J)$ (J = 0,1,2) energy transfer.

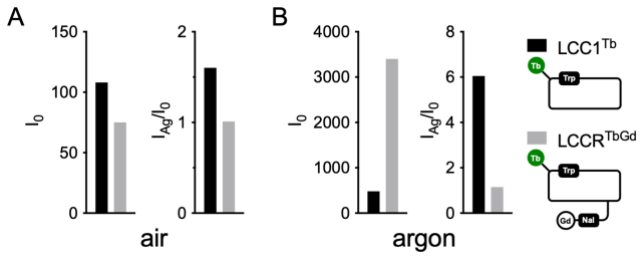

Figure 7. Comparison of time-gated Tb^{3+} emission (λ_{ex} = 280 nm, delay time = 100 µs) of **LCCR^{TbGd}** (grey) and **LCC1^{Tb}** (black) in (A) aerobic and (B) anaerobic conditions. I_0 corresponds to the intensity of the free probe and I_{Ag}/I_0, the Ag^+-induced luminescence enhancement. Solutions were prepared in HEPES buffer (10 mM, pH 7.5).

As mentioned above, the Eu^{3+} excitation spectrum is red-shifted upon Cu^+ or Ag^+ binding for **LCCR^{TbEu}**, indicating that part of the Eu^{3+} luminescence originates from photons absorbed by the tryptophan. Hence, tryptophan(S_1) → tryptophan(T_1) → $Tb^{3+}(^5D_4)$ ⇆ naphthalene(T_1) → $Eu^{3+}(^5D_J)$ (pathway *A*) is a likely pathway for the sensitization of Eu^{3+} from photons absorbed by the tryptophan. However, alternative pathways involving energy transfer from the tryptophan to the naphthalene, i.e. tryptophan(S_1) → tryptophan(T_1) → naphthalene(T_1) → $Eu^{3+}(^5D_J)$ (pathway *B*), tryptophan(S_1) → naphthalene(S_1) → naphthalene(T_1) → $Eu^{3+}(^5D_J)$ (pathway *C*) or tryptophan(S_1) → naphthalene(T_1) → $Eu^{3+}(^5D_J)$ (pathway *D*), cannot be ruled out. Therefore, we studied the **LCCR^{GdEu}** variant that lacks the Tb^{3+} emitter. Should pathway *A* be the only effective pathway for **LCCR^{TbEu}** for sensitization of Eu^{3+} from photons absorbed by the tryptophan, Eu^{3+} emission of **LCCR^{GdEu}** would not vary upon Ag^+ or Cu^+ binding because the Tb^{3+} relay is missing. Both metal-free probes show somewhat similar Eu^{3+} emission intensity, both in aerobic or anaerobic conditions as well as Eu^{3+} enhancement upon metal binding (Figure 8). As for **LCCR^{TbEu}**, the Eu^{3+} excitation spectrum of **LCCR^{GdEu}** is red-shifted upon Cu^+ or Ag^+ binding (Figure S13 of SI), indicating that the enhancement of Eu^{3+} emission is associated to the cation-π interaction established between the tryptophan and the metal cation. Therefore, the Eu^{3+} emission originates in part from photons absorbed by the tryptophan. This is only possible when considering that EET between the tryptophan and the naphthalene takes place. More importantly, this is an effective process since both probes display similar intensities of Eu^{3+} emission. As a consequence, we cannot exclude that either one or several pathways between *B*, *C* and *D* play a major role in the response of **LCCR^{TbEu}**.

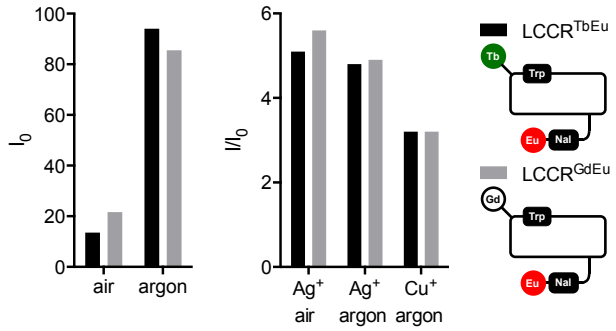

Figure 8. Comparison of time-gated Eu^{3+} emission (λ_{ex} = 280 nm, delay time = 100 µs) of **LCCΔ^{GdEu}** (grey) and **LCCR^{Tb}** (black) in aerobic or anaerobic conditions. I_0 corresponds to the intensity of the free probe and I/I_0, the Ag^+ or Cu^+-induced luminescence enhancement. Solutions were prepared in HEPES buffer (10 mM, pH 7.5), containing NH_2OH (20 mM) in the case of the Cu^+ sample.

In order to identify a possible EET between tryptophan and naphthalene, **LCCR^{GdGd}**, in which both Tb^{3+} and Eu^{3+} are replaced by Gd^{3+}, studies were performed at the nanosecond and microsecond timescales using streak-camera detection. Investigation at the nanosecond timescale was not informative. The fluorescence decay was biexponential with decay time constants of ca. 2 and 7 ns for both **LCCR^{GdGd}** and **Ag·LCCR^{GdGd}**. No evidence of EET from a tryptophan(S_1) state (or naphthalene) could be found. This is not surprising since in these systems, fluorescent species are those in which tryptophan is not involved in a cation-π interaction. Indeed, Cu or Ag-bound probes of the **LCC1^{Tb}** family exist in two forms in equilibrium: one with the tryptophan engaged in a cation-π that is not fluorescent, and the other one, where the tryptophan is not engaged in the cation-π interaction, which is fluorescent.[20,21] At the microsecond timescale, a broad emission is detected in the 400-700 nm range in the case of metal-free **LCCR^{GdGd}** that decays monoexponentially with a time constant of 46 ± 2 µs, homogenous over the whole spectral range (Figure S14 in SI). This emission could correspond to naphthalene triplet emission[50] since tryptophan emission was never detected in the Cu- or Ag-free forms for compounds of the **LCC1^{Tb}** family.[20,21] Addition of Ag^+ red-shifts the emission and the decay time is not homogenous on the whole 400-700 nm range, which could account for additional tryptophan(T_1) emission. At 450 nm, the decay could be fit with a monoexponential and a time constant of 25 µs, while at 570 nm, a monoexponential with a longer 49 µs decay time could be satisfyingly used to fit the decay. Due to the similarity and broadness of tryptophan and naphthalene triplet emission spectra, no conclusion could be drawn from these experiments. Study of **LCCR^{GdEu}** or **LCCR^{TbEu}** with streak-camera detection was not informative either.

Conclusion

We previously described a family of bioinspired Cu^+-responsive luminescent probes based on the copper-binding site of the protein CusF and on a Tb^{3+} complex as emitter. A tryptophan served as a Cu^+ ligand as well as an antenna for Tb^{3+} sensitization. Establishment of a cation-π interaction between Cu^+ and the tryptophan was responsible for an increase of Tb^{3+} emission upon copper binding. In this article, we have shown that a ratiometric Cu^+ (or Ag^+) luminescent probe, **LCCR^{TbEu}**, can be obtained by adding a naphthalene / Eu^{3+} complex pair to the previous probes. Upon Cu^+ binding, the intensity of Tb^{3+} and Eu^{3+} emission increases 1.35 and 3.15 times, respectively. The Tb^{3+} luminescence lifetime is also affected by copper binding. Therefore, **LCCR^{TbEu}** can be used for ratiometric detection of Cu^+ by monitoring either spectral changes (the relative Eu^{3+} / Tb^{3+} intensity) or Tb^{3+} lifetime change. In order to understand the mechanism responsible for this response, we have synthesized and studied several variants lacking one or several of the chromophores of the systems among naphthalene, Tb^{3+} and Eu^{3+}. It appears that tryptophan-to-Eu^{3+} EET as well as Tb^{3+}-to-Eu^{3+} EET are not efficient processes in this system. Naphthalene, which has a triplet excited state almost isoenergetic with the $Tb^{3+}(^5D_4)$ excited state, plays an important role in the system because forward and backward EET between $Tb^{3+}(^5D_4)$ and naphthalene(T_1) is occurring and seems to be responsible for the relative intensity of Tb^{3+} and Eu^{3+} emission. In fact, with **LCCR^{TbEu}**, it is likely that : (i) the cation-π interaction established upon Cu^+ binding causes the global increase of Ln^{3+} emission by increasing the efficiency of electronic energy transferred from the tryptophan to the Tb^{3+} or to the naphthalene and (ii) that the relative rate constants of energy transfer between the naphthalene and Tb^{3+} (forward and back) as well as Eu^{3+} (forward) regulates the relative proportion of Tb^{3+} and Eu^{3+} emission. The change in this

proportion is likely to be due to conformational changes arising upon Cu^+ binding that change the distance between naphthalene and the Ln^{3+}. Indeed, **LCCR^{TbEu}**, which comprises two antenna / Ln^{3+} pairs, can be viewed as a resonant system whose equilibrium point is displaced by copper binding. Hence, the strategy of using two antenna / Ln^{3+} pairs appears easy to implement and attractive for the design of ratiometric systems that could be used in many instances, notably in chemosensoring applications.

Acknowledgements

Authors acknowledge the Agence Nationale de la Recherche (ANR-12-BS07-0012), the Labex ARCANE and CBH-EUR-GS (ANR-17-EURE-0003) for financial support.

Supporting information available

Procedures for the synthesis of **LCCR^{Ln1Ln2}** and **LCCΔ ^{Ln1Ln2}** and spectroscopic characterization including sample preparation, absorption, fluorescence titration of **LCCR^{TbEu}** by Cu^+, determination of hydration number; determination of binding constants, excitation spectra of **LCCR^{TbEu}** and **LCCR^{GdEu}**, time-gated emission of **LCCR^{TbEu}**, Ag·**LCCR^{TbEu}** and Cu·**LCCR^{TbEu}** and time-resolved emission spectroscopy of **LCCR^{GdGd}**.

References

(1) Vest, K. E.; Hashemi, H. F.; Cobine, P. A. The Copper Metallome in Eukaryotic Cells. In *Metallomics and the Cell*; Banci, L., Ed.; Metal Ions in Life Sciences; Springer Netherlands, 2013; pp 451–478. https://doi.org/10.1007/978-94-007-5561-1_13.
(2) Rensing, C.; McDevitt, S. F. The Copper Metallome in Prokaryotic Cells. In *Metallomics and the Cell*; Banci, L., Ed.; Metal Ions in Life Sciences; Springer Netherlands, 2013; pp 417–450. https://doi.org/10.1007/978-94-007-5561-1_12.
(3) Kim, B.-E.; Nevitt, T.; Thiele, D. J. Mechanisms for Copper Acquisition, Distribution and Regulation. *Nat. Chem. Biol.* **2008**, *4* (3), 176–185. https://doi.org/10.1038/nchembio.72.
(4) Lutsenko, S. Copper Trafficking to the Secretory Pathway. *Metallomics* **2016**, *8* (9), 840–852. https://doi.org/10.1039/C6MT00176A.
(5) Vulpe, C.; Levinson, B.; Whitney, S.; Packman, S.; Gitschier, J. Isolation of a Candidate Gene for Menkes Disease and Evidence That It Encodes a Copper-Transporting Atpase. *Nature Genet.* **1993**, *3* (1), 7–13. https://doi.org/10.1038/ng0193-7.
(6) Bull, P. C.; Thomas, G. R.; Rommens, J. M.; Forbes, J. R.; Cox, D. W. The Wilson Disease Gene Is a Putative Copper Transporting P-Type Atpase Similar to the Menkes Gene. *Nature Genet.* **1993**, *5* (4), 327–337. https://doi.org/10.1038/ng1293-327.
(7) Atrian-Blasco, E.; Gonzalez, P.; Santoro, A.; Alies, B.; Faller, P.; Hureau, C. Cu and Zn Coordination to Amyloid Peptides: From Fascinating Chemistry to Debated Pathological Relevance. *Coord. Chem. Rev.* **2018**, *371*, 38–55. https://doi.org/10.1016/j.ccr.2018.04.007.
(8) Brady, D. C.; Crowe, M. S.; Turski, M. L.; Hobbs, G. A.; Yao, X.; Chaikuad, A.; Knapp, S.; Xiao, K.; Campbell, S. L.; Thiele, D. J.; Counter, C. M. Copper Is Required for Oncogenic BRAF Signalling and Tumorigenesis. *Nature* **2014**, *509* (7501), 492–496. https://doi.org/10.1038/nature13180.
(9) Fahrni, C. J. Synthetic Fluorescent Probes for Monovalent Copper. *Curr. Opin. Chem. Biol.* **2013**, *17* (4), 656–662. https://doi.org/10.1016/j.cbpa.2013.05.019.
(10) Aron, A. T.; Ramos-Torres, K. M.; Cotruvo, J. A.; Chang, C. J. Recognition- and Reactivity-Based Fluorescent Probes for Studying Transition Metal Signaling in Living Systems. *Acc. Chem. Res.* **2015**, *48* (8), 2434–2442. https://doi.org/10.1021/acs.accounts.5b00221.
(11) Joseph A. Cotruvo, J.; Aron, A. T.; Ramos-Torres, K. M.; Chang, C. J. Synthetic Fluorescent Probes for Studying Copper in Biological Systems. *Chem. Soc. Rev.* **2015**, *44* (13), 4400–4414. https://doi.org/10.1039/C4CS00346B.
(12) Morgan, M. T.; McCallum, A. M.; Fahrni, C. J. Rational Design of a Water-Soluble, Lipid-Compatible

Fluorescent Probe for Cu(I) with Sub-Part-per-Trillion Sensitivity. *Chem. Sci.* **2016**, *7* (2), 1468–1473. https://doi.org/10.1039/C5SC03643G.
(13) Jia, S.; Ramos-Torres, K. M.; Kolemen, S.; Ackerman, C. M.; Chang, C. J. Tuning the Color Palette of Fluorescent Copper Sensors through Systematic Heteroatom Substitution at Rhodol Cores. *ACS Chem. Biol.* **2018**, *13* (7), 1844–1852. https://doi.org/10.1021/acschembio.7b00748.
(14) Domaille, D. W.; Zeng, L.; Chang, C. J. Visualizing Ascorbate-Triggered Release of Labile Copper within Living Cells Using a Ratiometric Fluorescent Sensor. *J. Am. Chem. Soc.* **2010**, *132* (4), 1194–1195. https://doi.org/10.1021/ja907778b.
(15) Shen, C.; Kolanowski, J. L.; Tran, C. M.-N.; Kaur, A.; Akerfeldt, M. C.; Rahme, M. S.; Hambley, T. W.; New, E. J. A Ratiometric Fluorescent Sensor for the Mitochondrial Copper Pool. *Metallomics* **2016**, *8* (9), 915–919. https://doi.org/10.1039/C6MT00083E.
(16) Chung, C. Y.-S.; Posimo, J. M.; Lee, S.; Tsang, T.; Davis, J. M.; Brady, D. C.; Chang, C. J. Activity-Based Ratiometric FRET Probe Reveals Oncogene-Driven Changes in Labile Copper Pools Induced by Altered Glutathione Metabolism. *Proc. Natl. Acad. Sci. U. S. A.* **2019**, *116* (37), 18285–18294. https://doi.org/10.1073/pnas.1904610116.
(17) Isaac, M.; Raibaut, L.; Cepeda, C.; Roux, A.; Boturyn, D.; Eliseeva, S. V.; Petoud, S.; Sénèque, O. Luminescent Zinc Fingers: Zn-Responsive Neodymium Near-Infrared Emission in Water. *Chem.-Eur. J.* **2017**, *23* (46), 10992–10996. https://doi.org/10.1002/chem.201703089.
(18) Fremy, G.; Raibaut, L.; Cepeda, C.; Sanson, M.; Boujut, M.; Sénèque, O. A Novel DOTA-like Building Block with a Picolinate Arm for the Synthesis of Lanthanide Complex-Peptide Conjugates with Improved Luminescence Properties. *J. Inorg. Biochem.* **2020**, *213*, 111257. https://doi.org/10.1016/j.jinorgbio.2020.111257.
(19) Cepeda, C.; Raibaut, L.; Fremy, G.; Eliseeva, S. V.; Romieu, A.; Pecaut, J.; Boturyn, D.; Petoud, S.; Seneque, O. Using Native Chemical Ligation for Site-Specific Synthesis of Hetero-Bis-Lanthanide Peptide Conjugates: Application to Ratiometric Visible or Near-Infrared Detection of Zn2+. *Chem.-Eur. J.* **2020**, *26* (59), 13476–13483. https://doi.org/10.1002/chem.202002708.
(20) Isaac, M.; Denisov, S. A.; Roux, A.; Imbert, D.; Jonusauskas, G.; McClenaghan, N. D.; Sénèque, O. Lanthanide Luminescence Modulation by Cation–π Interaction in a Bioinspired Scaffold: Selective Detection of Copper(I). *Angew. Chem., Int. Ed.* **2015**, *54* (39), 11453–11456. https://doi.org/10.1002/anie.201505733.
(21) Roux, A.; Isaac, M.; Chabert, V.; Denisov, S. A.; McClenaghan, N. D.; Sénèque, O. Influence of Amino Acid Sequence in a Peptidic Cu+-Responsive Luminescent Probe Inspired by the Copper Chaperone CusF. *Org. Biomol. Chem.* **2018**, *16* (31), 5626–5634. https://doi.org/10.1039/C8OB01044G.
(22) Raibaut, L.; Vasseur, W.; Shimberg, G. D.; Saint-Pierre, C.; Ravanat, J.-L.; Michel, S. L. J.; Sénèque, O. Design of a Synthetic Luminescent Probe from a Biomolecule Binding Domain: Selective Detection of AU-Rich MRNA Sequences. *Chem. Sci.* **2017**, *8* (2), 1658–1664. https://doi.org/10.1039/C6SC04086A.
(23) Montgomery, C. P.; Murray, B. S.; New, E. J.; Pal, R.; Parker, D. Cell-Penetrating Metal Complex Optical Probes: Targeted and Responsive Systems Based on Lanthanide Luminescence. *Acc. Chem. Res.* **2009**, *42* (7), 925–937. https://doi.org/10.1021/ar800174z.
(24) Heffern, M. C.; Matosziuk, L. M.; Meade, T. J. Lanthanide Probes for Bioresponsive Imaging. *Chem. Rev.* **2014**, *114* (8), 4496–4539. https://doi.org/10.1021/cr400477t.
(25) Sy, M.; Nonat, A.; Hildebrandt, N.; Charbonnière, L. J. Lanthanide-Based Luminescence Biolabelling. *Chem. Commun.* **2016**, *52* (29), 5080–5095. https://doi.org/10.1039/C6CC00922K.
(26) Bünzli, J.-C. G. Lanthanide Light for Biology and Medical Diagnosis. *J. Lumin.* **2016**, *170*, 866–878. https://doi.org/10.1016/j.jlumin.2015.07.033.
(27) Jin, G.-Q.; Ning, Y.; Geng, J.-X.; Jiang, Z.-F.; Wang, Y.; Zhang, J.-L. Joining the Journey to near Infrared (NIR) Imaging: The Emerging Role of Lanthanides in the Designing of Molecular Probes. *Inorg. Chem. Front.* **2020**, *7* (2), 289–299. https://doi.org/10.1039/C9QI01132C.
(28) Parker, D.; Fradgley, J. D.; Wong, K.-L. The Design of Responsive Luminescent Lanthanide Probes and Sensors. *Chem. Soc. Rev.* **2021**, *50* (14), 8193–8213. https://doi.org/10.1039/D1CS00310K.
(29) Bodman, S. E.; Butler, S. J. Advances in Anion Binding and Sensing Using Luminescent Lanthanide Complexes. *Chem. Sci.* **2021**, *12* (8), 2716–2734. https://doi.org/10.1039/D0SC05419D.
(30) Shuvaev, S.; Starck, M.; Parker, D. Responsive, Water-Soluble Europium(III) Luminescent Probes. *Chem.-Eur. J.* **2017**, *23* (42), 9974–9989. https://doi.org/10.1002/chem.201700567.
(31) Bradberry, S. J.; Savyasachi, A. J.; Martinez-Calvo, M.; Gunnlaugsson, T. Development of Responsive Visibly and NIR Luminescent and Supramolecular Coordination Self-Assemblies Using Lanthanide Ion Directed Synthesis. *Coord. Chem. Rev.* **2014**, *273–274*, 226–241. https://doi.org/10.1016/j.ccr.2014.03.023.
(32) Kim, E.-H.; Rensing, C.; McEvoy, M. M. Chaperone-Mediated Copper Handling in the Periplasm. *Nat. Prod. Rep.* **2010**, *27* (5), 711–719. https://doi.org/10.1039/b906681k.
(33) Delmar, J. A.; Su, C.-C.; Yu, E. W. Structural Mechanisms of Heavy-Metal Extrusion by the Cus Efflux

System. *Biometals* **2013**, *26* (4), 593–607. https://doi.org/10.1007/s10534-013-9628-0.
(34) Davis, A. V.; O'Halloran, T. V. A Place for Thioether Chemistry in Cellular Copper Ion Recognition and Trafficking. *Nat. Chem. Biol.* **2008**, *4* (3), 148–151. https://doi.org/10.1038/nchembio0308-148.
(35) Ramos-Torres, K. M.; Kolemen, S.; Chang, C. J. Thioether Coordination Chemistry for Molecular Imaging of Copper in Biological Systems. *Isr. J. Chem.* **2016**, *56* (9–10), 724–737. https://doi.org/10.1002/ijch.201600023.
(36) Xue, Y.; Davis, A. V.; Balakrishnan, G.; Stasser, J. P.; Staehlin, B. M.; Focia, P.; Spiro, T. G.; Penner-Hahn, J. E.; O'Halloran, T. V. Cu(I) Recognition via Cation-Pi and Methionine Interactions in CusF. *Nat. Chem. Biol.* **2008**, *4* (2), 107–109. https://doi.org/10.1038/nchembio.2007.57.
(37) Horrocks, W. D.; Bolender, J. P.; Smith, W. D.; Supkowski, R. M. Photosensitized near Infrared Luminescence of Ytterbium(III) in Proteins and Complexes Occurs via an Internal Redox Process. *J. Am. Chem. Soc.* **1997**, *119* (25), 5972–5973.
(38) Quici, S.; Cavazzini, M.; Raffo, M. C.; Botta, M.; Giovenzana, G. B.; Ventura, B.; Accorsi, G.; Barigelletti, F. Luminescence Properties and Solution Dynamics of Lanthanide Complexes Composed by a Macrocycle Hosting Site and Naphthalene or Quinoline Appended Chromophore. *Inorg. Chim. Acta* **2007**, *360* (8), 2549–2557. https://doi.org/10.1016/j.ica.2006.12.040.
(39) Routledge, J. D.; Jones, M. W.; Faulkner, S.; Tropiano, M. Kinetically Stable Lanthanide Complexes Displaying Exceptionally High Quantum Yields upon Long-Wavelength Excitation: Synthesis, Photophysical Properties, and Solution Speciation. *Inorg. Chem.* **2015**, *54* (7), 3337–3345. https://doi.org/10.1021/ic503049m.
(40) Sørensen, T. J.; Kenwright, A. M.; Faulkner, S. Bimetallic Lanthanide Complexes That Display a Ratiometric Response to Oxygen Concentrations. *Chem. Sci.* **2015**, *6* (3), 2054–2059. https://doi.org/10.1039/C4SC03827D.
(41) Ollivier, N.; Dheur, J.; Mhidia, R.; Blanpain, A.; Melnyk, O. Bis(2-Sulfanylethyl)Amino Native Peptide Ligation. *Org. Lett.* **2010**, *12* (22), 5238–5241. https://doi.org/10.1021/ol102273u.
(42) Boll, E.; Ebran, J.-P.; Drobecq, H.; El-Mahdi, O.; Raibaut, L.; Ollivier, N.; Melnyk, O. Access to Large Cyclic Peptides by a One-Pot Two-Peptide Segment Ligation/Cyclization Process. *Org. Lett.* **2015**, *17* (1), 130–133. https://doi.org/10.1021/ol503359w.
(43) Agouridas, V.; El Mahdi, O.; Diemer, V.; Cargoët, M.; Monbaliu, J.-C. M.; Melnyk, O. Native Chemical Ligation and Extended Methods: Mechanisms, Catalysis, Scope, and Limitations. *Chem. Rev.* **2019**, *119* (12), 7328–7443. https://doi.org/10.1021/acs.chemrev.8b00712.
(44) Isaac, M.; Pallier, A.; Szeremeta, F.; Bayle, P.-A.; Barantin, L.; Bonnet, C. S.; Sénèque, O. MRI and Luminescence Detection of Zn2+ with a Lanthanide Complex–Zinc Finger Peptide Conjugate. *Chem. Commun.* **2018**, *54* (53), 7350–7353. https://doi.org/10.1039/C8CC04366C.
(45) Montalti, M.; Credi, A.; Prodi, L.; Gandolfi, M. T. Photophysical Properties of Organic Compounds. In *Handbook of Photochemistry, 3rd Ed.*; CRC Press: Boca Raton, 2006.
(46) Kai, Y.; Imakubo, K. Temperature Dependence of the Phosphorescence Lifetimes of Heterogeneous Tryptophan Residues in Globular Proteins Between 293 and 77 K. *Photochem. Photobiol.* **1979**, *29* (2), 261–265. https://doi.org/10.1111/j.1751-1097.1979.tb07047.x.
(47) Mazhul', V. M.; Timoshenko, A. V.; Zaitseva, E. M.; Loznikova, S. G.; Halets, I. V.; Chernovets, T. S. Room Temperature Tryptophan Phosphorescence of Proteins in the Composition of Biological Membranes and Solutions. In *Reviews in Fluorescence*; Springer: Dordrecht, 2008; pp 37–67.
(48) Masuhara, H.; Shioyama, H.; Saito, T.; Hamada, K.; Yasoshima, S.; Mataga, N. Fluorescence Quenching Mechanism of Aromatic-Hydrocarbons by Closed-Shell Heavy-Metal Ions in Aqueous and Organic Solutions. *J. Phys. Chem.* **1984**, *88* (24), 5868–5873. https://doi.org/10.1021/j150668a026.
(49) Zaïm, A.; Eliseeva, S. V.; Guénée, L.; Nozary, H.; Petoud, S.; Piguet, C. Lanthanide-to-Lanthanide Energy-Transfer Processes Operating in Discrete Polynuclear Complexes: Can Trivalent Europium Be Used as a Local Structural Probe? *Chem.-Eur. J.* **2014**, *20* (38), 12172–12182. https://doi.org/10.1002/chem.201403206.
(50) Isaac, M.; Denisov, S. A.; McClenaghan, N. D.; Sénèque, O. Bioinspired Luminescent Europium-Based Probe Capable of Discrimination between Ag+ and Cu+. *Inorg. Chem.* **2021**, *60* (14), 10791–10798. https://doi.org/10.1021/acs.inorgchem.1c01486.